International Journal of Advanced Trends in Engineering and Management
(ISSN 2583-7052)
Vol. V, No. 02, pp. 32-40, February

Artificial Rabbits Optimized Mamba State Space and Temporal Convolutional Network for Intelligent Marine Engine Fault Diagnosis

Pradheep T Rajan B[3]
[3]Assistant Professor, Department of Electronics and Communication Engineering,
Francis Xavier Engineering College, Tirunelveli, Tamil Nadu, India.

ABSTRACT: Early diagnosis and accurate detection of Marine Engine Faults (MEF) is essential for improving vessel safety, operational reliability, maintenance efficiency, and reducing unexpected downtime. In this paper an Artificial Rabbits Optimized Mamba State Space and Temporal Convolutional Network (ARO-MSS–TCN) framework is proposed for intelligent MEF diagnosis. Data processing based on Min–Max normalization used to improve data consistency. Data visualization is then implemented to identify important patterns and variations in engine operating conditions, followed by training and testing data splitting. The proposed hybrid model combines the MSS model for efficiently learning long-range temporal dependencies with the TCN for extracting local and multiscale temporal features from engine signals. Furthermore, the ARO algorithm is used to optimize the model parameters, thereby improving classification performance as well as convergence. The proposed framework is implemented in Python software using marine engine performance & fault diagnosis dataset and it is estimated with accuracy, precision, recall, F1-score, as well as ROC-AUC metrics of 98%. The resulting intelligent diagnostic framework provides an effective and computationally efficient approach for reliable MEF detection and support predictive maintenance and intelligent marine machinery management. Future work, focus on with larger datasets from different marine engines and vessels to develop its simplification in marine locations.

Keywords: Marine Engine Faults Diagnosis, Artificial Rabbits Optimization, Mamba State Space, Temporal Convolutional Network.

1. Introduction

The safety and reliable operation of ME, which serve as the primary power source for ships, is essential for safe and efficient maritime transportation [1]. With advances in science and technology, ME have become more efficient and powerful; however, their internal structures have also become increasingly complex [2-3]. Moreover, ME [4] operate under harsh conditions, making them susceptible to problems like component wear, inadequate cooling, and other mechanical faults [5]. Such failures threaten the safety of the vessel and its crew, cause operational disruptions and financial losses, and increase environmental pollution [6-7]. Therefore, fast and accurate fault diagnosis of ME is important for maintaining vessel safety, reliability, and operational efficiency.

2. Related works

Several techniques are utilized for MEF diagnosis in [8] Improved Convolutional Neural Network (ICNN) with Meta-ACON and AdamP optimization algorithm, through Label Smoothing Regularization (LSR) is used. LSR reduces overconfidence in predictions and improves generalization. However, performance depends on properly selecting learning rate. Consequently, in [9] Constrained Penalty Leech Algorithm (CPLA) with Improved Complete Ensemble Empirical Mode Decomposition with Adaptive Noise (ICEEMDAN) is used for MEF diagnosis. CPLA identify suitable ICEEMDAN parameters more effectively. Nevertheless, multiple decomposition and optimization iterations increase execution time. Additionally, in [10] CNN with Bidirectional Gated Recurrent Unit (BiGRU). The CNN extracts important local patterns and features from marine diesel engine monitoring signals. Nonetheless, unsuitable when future observations are unavailable during online prediction. Furthermore, in [11] Long Short-Term Memory (LSTM) with Improved Beluga Whale Optimization (IBWO) algorithm is used for MEF diagnosis. It handles complex and time-varying ME operating conditions. Nevertheless, require much iteration before obtaining suitable LSTM parameters. Moreover, in [12] Support Vector Machine (SVM) with Improved Sparrow Search Algorithm (ISSA) is used for fault diagnosis. SVM perform well even when the training dataset is relatively small. However, SVM become computationally expensive when the number of training samples becomes very large.

2.1 Problem statement

Existing DL and ML techniques have limited capability in capturing long-term temporal dependences as well as local multi scale fault characteristics. To overcome these challenges, this paper proposes an ARO-MSS–TCN organization to improve the reliability and accuracy of MEF analysis.

2.2 Research Contribution

Data processing based on Min–Max normalization and data visualization are used to improve data consistency, and identify meaningful variations in ME operating conditions. A novel ARO-MSS–TCN model is proposed for accurate and intelligent MEF diagnosis by combining MSS and TCN. The ARO algorithm is integrated to optimize important model parameters, reducing manual parameter selection and improving convergence and classification performance.

3. Proposed Methodology

The collected numerical data are cleaned then transformed by Min–Max normalization to improve data consistency. Data visualization is performed to examine the distribution, variation, and relationships among engine parameters and identify patterns related through different fault conditions. The processed dataset is distributed into training then testing sets to train the proposed technique as well as evaluate its generalization capability. The proposed MSS component learns long-range temporal dependencies from sequential marine engine signals. Then the TCN extracts local and multi scale temporal features using temporal convolution operations, complementing the long-range representations learned by MSS. The features learned by MSS and TCN are combined to form a more informative representation of engine operating conditions, which is then used to classify different MEF types. Further to improve MSS–TCN model the ARO algorithm optimizes the important parameters to obtain an effective parameter configuration and improve classification accuracy and convergence. The block diagram for the proposed ARO-MSS–TCN technique is shown in fig.1.

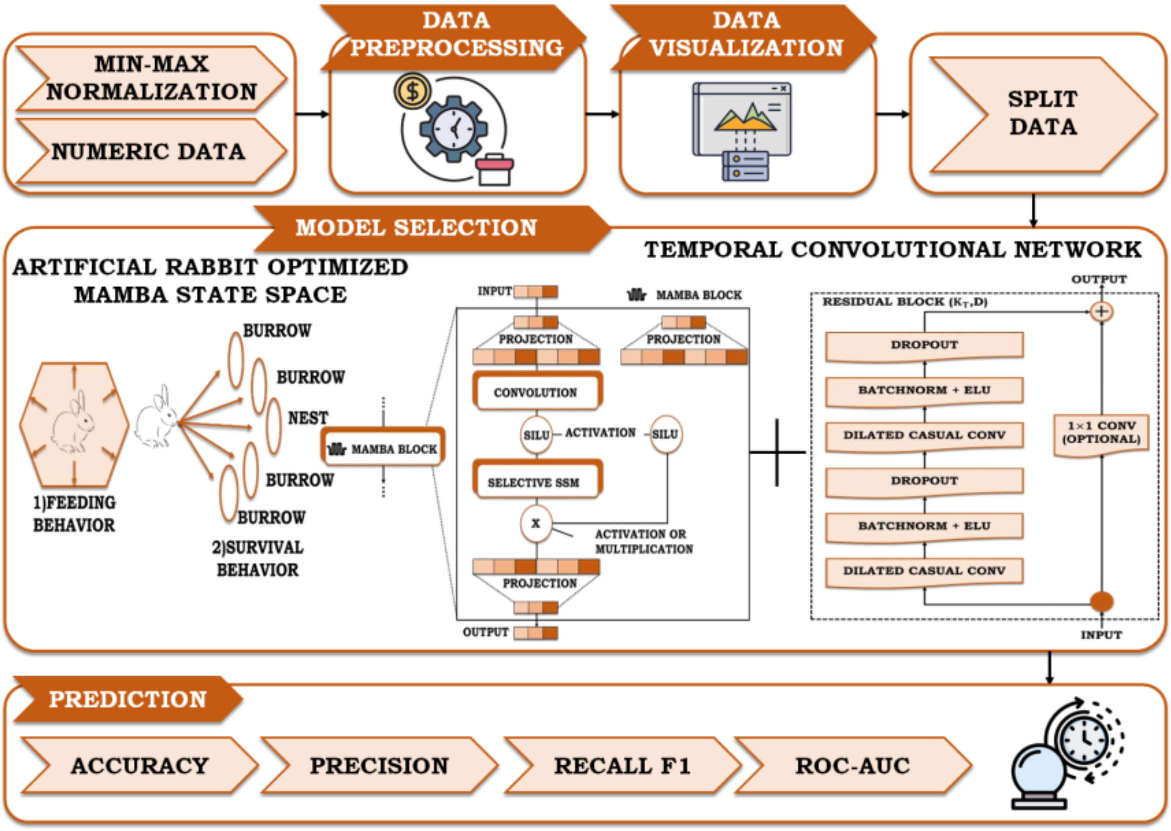

Figure 1: *Proposed block diagram for ABO-MSS-TCN*

3.1 Data Processing based on Mini-Max Normalization

Mini-Max normalization is used to improve data consistency, and facilitate efficient model training. Normalization converts these features into a common range, typically [0, 1],

$$X_{norm} = \frac{X - \bar{X}}{X_{max} - X_{min}} \quad (1)$$

Where, X_{norm} denotes normalized feature value, X represent original feature value, $\bar{X}$ indicates mean of the feature, X_{max}& X_{min} denotes maximum as well as minimum value of the feature. The normalized data is fed to data visualization

3.2 Data Visualization

Data visualization is used to understand the distribution and operating patterns of ME parameters. The histogram shows the distribution of engine sensor parameters like temperature, pressure, speed, and vibration. The correlation heat map indicates the relationships among engine parameters and identify strongly correlated features. Fault-class distribution demonstrates the number of samples belonging to normal and different fault categories. The visualized data is fed to Proposed ARO-MSS–TCN.

3.3 Proposed ARO-MSS–TCN

ARO-MSS

The MSS retain relevant historical information and discard irrelevant inputs for MEF diagnosis. The network first transforms the input features into latent representations, which are then processed through selective SS layers to capture both short-term as well as long-term pricing dependences. Figure 2 displays the proposed MSS. The learned feature representations are subsequently passed through fully connected layers to predict the TPP. The hidden state is efficient by the SS equation

$$h_t = Ah_{t-1} + Bx_t \quad (2)$$

Where, h_t denotes hidden state at time t, A indicates state transition matrix, B signifies input projection matrix, x_t represent input vector.

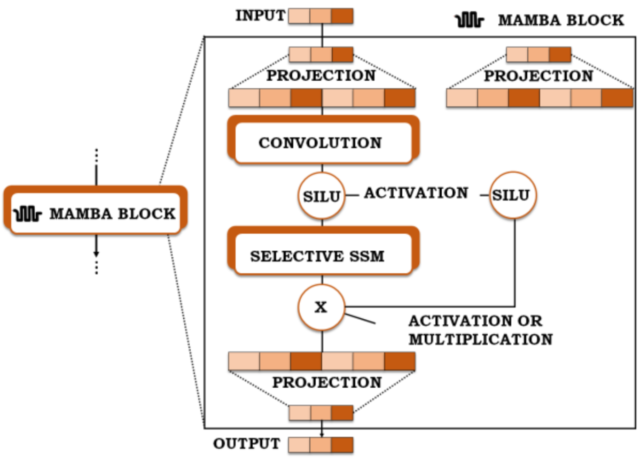

Figure 2: *Proposed MSS*

The Mamba network selectively updates its internal state by

$$h_t = f(h_{t-1}, x_t, \theta) \qquad (3)$$

Where, $f(\cdot)$ signifies the selective state-space function, θ denotes the learnable network parameters. The predicted MEF is calculated by

$$\hat{y} = Wh_t + b \qquad (4)$$

Where $\hat{y}$ indicates predicted MEF, W denotes output weight matrix, b represent bias vector. The lightweight architecture of Mamba significantly reduces computational complexity whereas maintaining high prediction accuracy.

TCN is used to extract local, short-term, and multi-scale temporal patterns from marine engine sensor signals. Figure 3 displays the TCN structure. This is important because faults like abnormal vibration, temperature changes, pressure fluctuations, and speed variations perform as temporal patterns in sequential engine measurements.

$$X = \{x_1, x_2, \ldots\ldots x_T\} \qquad (5)$$

Where, T indicates amount of time steps as well as x_T signifies the engine measurements at time$t$.

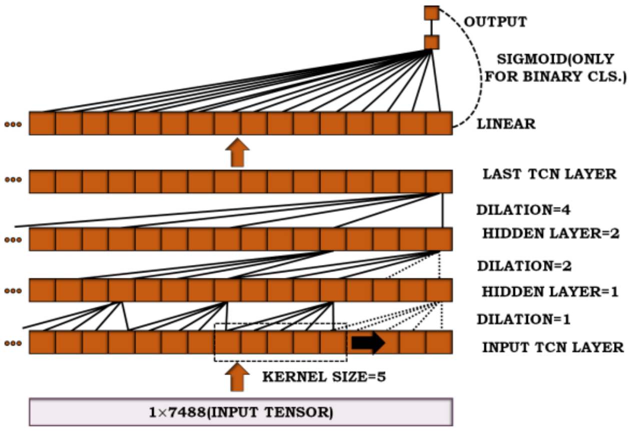

Figure 3: *TCN structure*

The dilated causal convolution operation across successive TCN layers mathematically said as

$$x_l^t = g\left(\sum_{k=0}^{k-1} w_l^k x_{(l-1)}^{(t-(k\times d))} + b_l\right) \qquad (6)$$

Wherever, x_l^t signifies the output of the neuron at time location t in the l^{th} layer, K designates the convolutional kernel size, w_l^k indicates the corresponding weight at location k, d represents dilation factor that determines the spacing between the kernel elements, and b_l signifies the bias term of the l^{th} layer.

ARO algorithm is inspired by the natural survival behaviour of rabbits, including detour foraging to search for food and random hiding in burrows to avoid predators. Figure 4 shows the flow chart for ABO. Each rabbit updates its position by moving toward a randomly selected rabbit whereas adding a random perturbation to maintain exploration and improve the search process.

$$Rabb_{new} = \vec{x}_j + R \times \left(\vec{x}_i - \vec{x}_j\right) + round\ (0.5 \times (0.05 + r_1)) \times n_1 \qquad (7)$$

$$R = L \times m \qquad (8)$$

$$L = \sin(2\pi r_2) \times \left(e - e^{\left(\frac{t-1}{T}\right)^2}\right) \qquad (9)$$

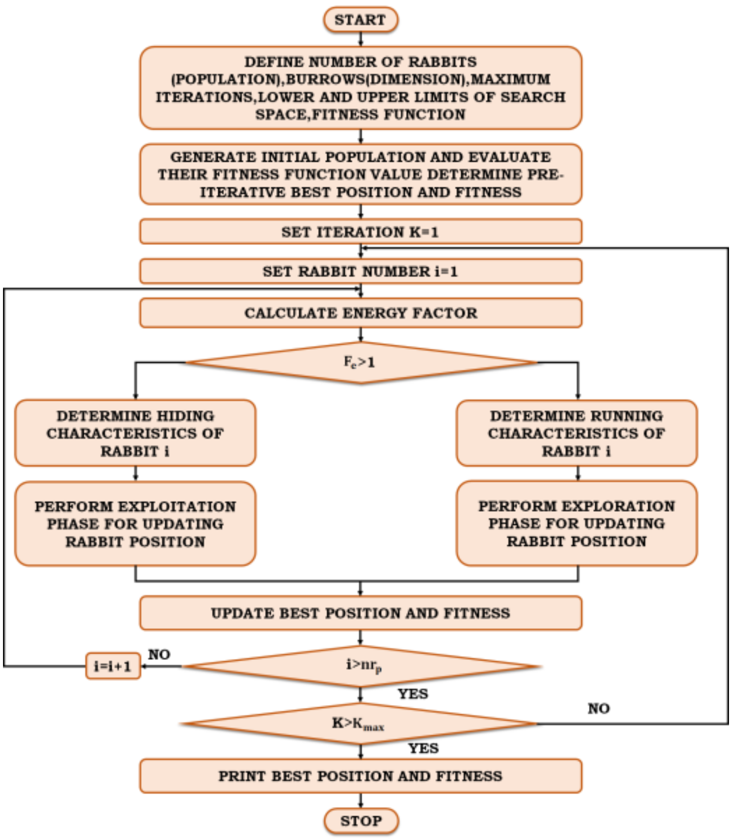

Figure 4: *Flowchart for ABO*

$$m(k) = \begin{cases} 0 & if\ k == g(l) \\ 1 & \end{cases} \quad (10)$$

$$Rabb_{new} = \vec{X}_i + R \times \left(r_1 \times (\vec{b}_{ir} - \vec{X}_i \right) \quad (11)$$

$$\vec{b}_{i,r} = \vec{X}_i + H \times g_r \times \vec{X}_i \quad (12)$$

Where, $Rabb_{new}$ indicates updated position of the i^{th} rabbit at iteration t, $(\vec{x}_i \,\&\, \vec{x}_j)$ denote the current positions of the i^{th} & j^{th} rabbits, respectively, at iteration t. The parameter n indicates population size, t signifies current repetition, T indicates maximum number of repetitions as well as d represents the dimensionality of the optimization problem. Thus by using the proposed technique the prediction accuracy is improved for MEF diagnosis.

4. Result and discussion

For MEF diagnosis the work is implemented in Python software using marine engine performance & fault diagnosis dataset. It have 10000 rows and 20 columns with X class of timestamp, and class Y of fault label. The class distribution 0 as normal operation, 1 as fuel injection fault, 2 as cylinder pressure loss, 3 as exhaust gas overheating, 4 as bearing/vibration fault, 5 as lubrication oil degradation, 6 as turbocharger failure and 7 as fixed fault

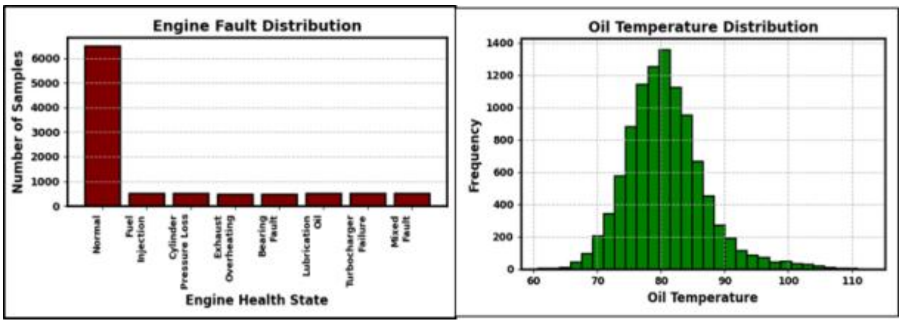

Figure 4: *Engine fault distribution & Oil temperature distribution*

Figure 5 shows engine fault distribution in this normal have roughly about 6,500 samples. The each fault types have about 500 samples these tracks seven distinct engine failures. The oil temperature distribution it is centered on a peak value near 80, which specifies that oil temperature observed, is nearly 80 degrees, representing the typical operating temperatures under normal conditions.

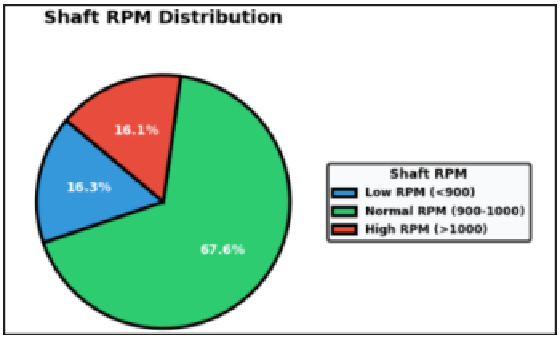

Figure 5: *Shaft RPM distribution*

Figure 6 shows the shaft RPM distribution. The low RPM (<900) have 16.3%, normal RPM (900-1000) have 67.6% and high RPM have the value of 16.1% low compared to other RPM.

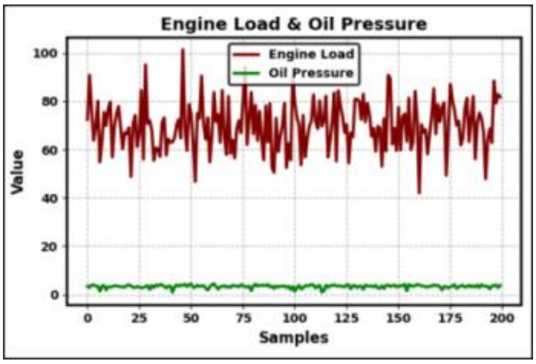

Figure 6: *Engine load & oil production*

Figure 7 displays engine load and oil production. The engine load is indicated in red line it is highly volatile data fluctuating heavily between roughly 40 and 100, maintaining an average value around 70. Oil pressure is indicated in green line very stable and low data, unevenly between 1 and 5 across all 200 samples.

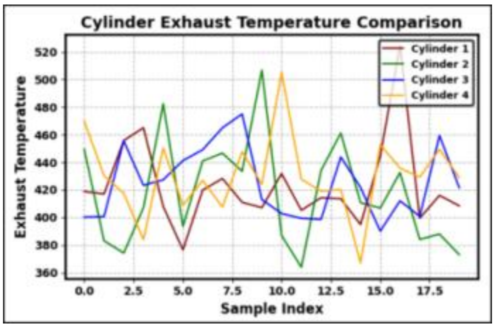

Figure 7: *Cylinder exhaust temperature comparison*

Figure8 displays cylinder exhaust temperature comparison. The temperatures vary among unevenly 360 and 520 units, with significant spikes and drops for individual cylinders, particularly around sample index 10 and 15.

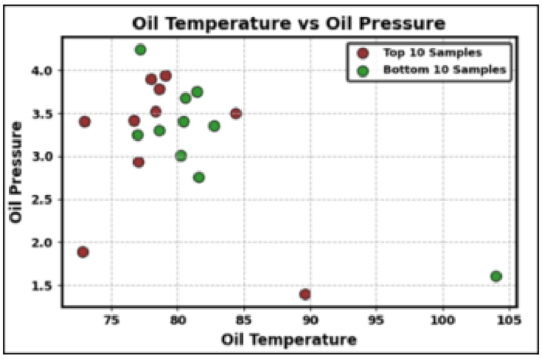

Figure 8: *Oil temperature vs oil pressure*

Figure 9 shows oil temperature vs oil pressure. The scatter plot displays that most samples are clustered around an oil temperature of 77–84 °C and an oil pressure of 3.0–4.0 bar, whereas a few outliers show abnormal engine operating conditions.

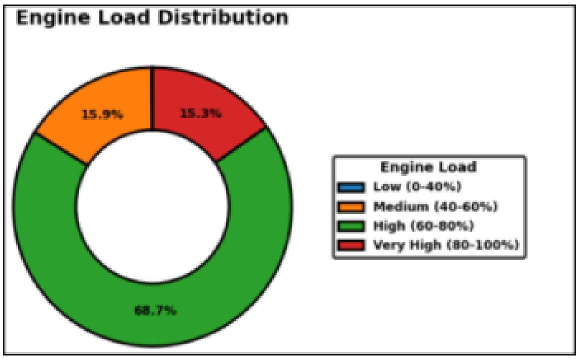

Figure 9: *Engine load distribution*

Figure 10 shows the engine load distribution. The medium (40-60%) have the value of 15.9%, high (60-80%) have the value of 68.7%, very high (80-100%) have the value of 15.3% respectively.

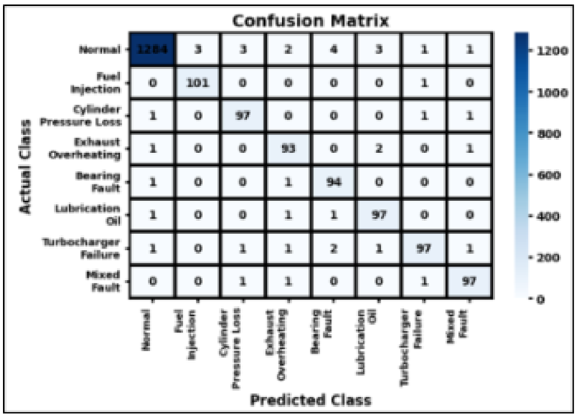

Figure 10: *Confusion matrix*

Figure 11 displays the confusion matrix for proposed ARO-MAA-TCN. It demonstrates excellent fault classification performance, correctly identifying 1,284 Normal, 101 Fuel Injection, 97 Cylinder Pressure Loss, 93 Exhaust Overheating, 94 Bearing Fault, 97 Lubrication Oil, 97 Turbocharger Failure, and 97 Mixed Fault samples for proposed ARO-MSS-TCN.

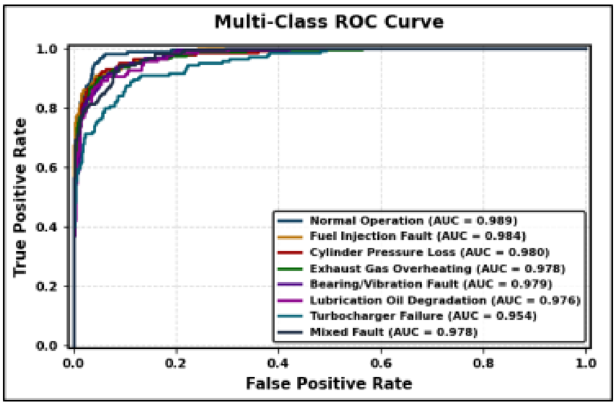

Figure 11: *Multi-class ROC curve*

Figure 12 shows multi-class ROC curve for proposed ARO-MSS-TCN. The normal operation, fuel injection and cylinder pressure loss have the AUC of 0.98, exhaust gas overheating, bearing/vibration fault, lubrication oil degradation and mixed fault have the AUC of 0.97 and turbocharger failure have the AUC of 0.95 respectively.

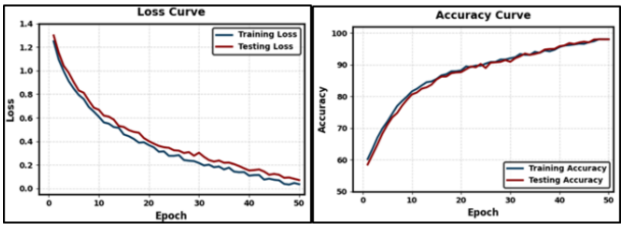

Figure 12: *Loss curve & Accuracy curve*

Figure 13 shows the loss curves it display stable model convergence, with the training loss decreasing from approximately 1.27 to 0.05indicating good learning performance and minimal overfitting. The accuracy curves for proposed ARO-MSS-TCN. It specify consistent learning performance, through the training accuracy growing from nearly 60% to 98% as well as the testing accuracy aggregate from about 58% to 98% over 50 epochs, representing excellent generalization and minimal overfitting.

Figure 13: *System model & fuel anomaly thermal spike & vibration alert.*

Figure 14 shows system model & fuel anomaly, thermal spike & vibration alert. The system model predicts the result class 0 as normal operation and fuel anomaly predict the result class 1 as fuel injection fault. Thermal spike predict the result class 3 as exhaust gas overheating and vibration alert predict the result class 4 as bearing/vibration fault.

Figure 14: *Vibration alert & oil critical, turbo fault & multi hazard.*

Figure 15 shows vibration alert & oil critical. The oil critical predict the result class 5 as lubrication oil degradation. The turbo fault predicts the result class 6 as turbocharger failure and multi hazard predict the result class 7 as mixed fault.

4.1 Comparison for proposed technique

In the comparison proposed ARO-MSS-TCN techniques is compared with the existing technique and have the accuracy, precision, recall as well as F1-score of 98% it is high compared with the existing techniques as presented in table 1.

Table 1: *Comparison with the proposed techniques*

Study	Precision (%)	Recall (%)	F1-score (%)
Wang et al [3]	94.1	94.1	94.1
Tian et al [6]	96.3	96.3	96.3
Proposed technique	98	98	98

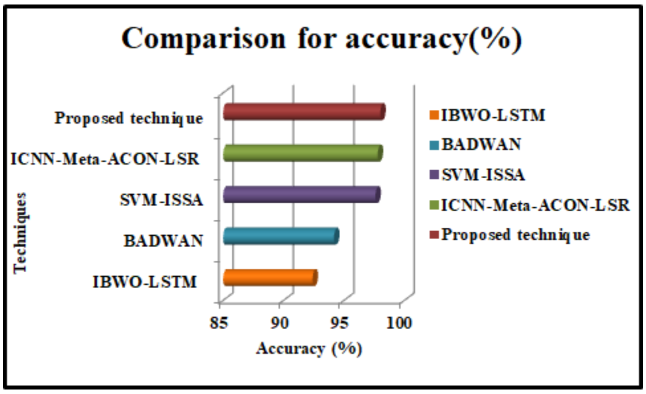

Figure 15: *Comparison for accuracy*

Figure 16 displays the comparison for accuracy. The accuracy for IBWO-LSTM [11] is 92.40%, BADWAN [3] is 94.17%, SVM-ISSA [8] is 97.6%, ICNN-Meta-ACON-LSR [12] is 97.78% and the proposed ARO-MSS-TCN have the higher accuracy of 98% compared with the existing techniques

5. Conclusion

In this paper an ARO-MSS–TCN framework is proposed for intelligent MEF diagnosis. The data processing based on Min–Max normalization improved data consistency, data visualization technique visualize the processed data and MSS-TCN architecture effectively learn both long-range temporal dependencies and local multi scale features from marine engine sensor data. The ARO algorithm further enhances the model by automatically optimizing its parameters, leading to improved convergence and classification performance. Experimental results is implemented in Python software demonstrate using the proposed framework it achieves 98% accuracy, precision, recall, F1-score, as well as ROC-AUC, confirming its ability to accurately classify different marine engine fault conditions.

References

1. Zhenguo Ji; Huibing Gan; Ben Liu, Year: 2023, “A deep learning-based fault warning model for exhaust temperature prediction and fault warning of marine diesel engine,” Journal of Marine Science and Engineering, Vol: 11, No: 8, pp. 1509.
2. Chaitanya Patil; Gerasimos Theotokatos; Konstantinos Tsitsilonis, Year: 2025, “Data-driven model for marine engine fault diagnosis using in-cylinder pressure signals,”Journal of Marine Engineering & Technology, Vol: 24, No: 1, pp. 70-82.
3. Longde Wang; Hui Cao; Zhichao Cui; Zeren Ai, Year: 2024, “A fault diagnosis method for marine engine cross working conditions based on transfer learning,” Journal of Marine Science and Engineering, Vol: 12, No: 2, pp. 270.
4. Yulong Su; Huibing Gan; Zhenguo J, Year: 2024, “Research on multi-parameter fault early warning for marine diesel engine based on PCA-CNN-BiLSTM, “Journal of Marine Science and Engineering, Vol: 12, No: 6, pp. 965.

5. Hui Ouyang; Weibo Li; Feng GAO; Kangzheng Huang; Peng Xiao, Year: 2024, "Research on fault diagnosis of ship diesel generator system based on IVY-RF,"Energies Vol: 17, No: 22, pp. 5799.
6. Xiaohe Tian; Huibing Gan; Yanlin Liu; Year: 2025, "Construction of knowledge graph for marine diesel engine faults based on deep learning methods," Journal of Marine Science and Engineering, Vol: 13, No: 4, pp. 693.
7. Defu Zhang; Yuxuan Song; Jianfeng Gao; Zhenyu Shen; Liangkuan Li; Anren Yao, Year: 2025, "Research on ship engine fuel consumption prediction algorithm based on adaptive optimization generative network," Journal of Marine Science and Engineering, Vol: 13, No: 6, pp. 1140.
8. Jihui Wang; Hui Cao; Zhichao Cui; Zeren Ai, Year: 2023, "Intelligent fault diagnosis of marine diesel engines based on efficient channel attention-improved convolutional neural networks," Processes, Vol: 11, No: 12, pp. 3360.
9. Haike Guo; Xiaoqiang Zhao, Year: 2026, "An interpretable fault diagnosis method for marine rotating machinery under strong noise based on constrained penalty leech algorithm optimized ICEEMDAN," Ocean Engineering, Vol: 344, pp. 123685.
10. Ben Liu; Huibing Gan; Dong Chen; Zepeng Shu, Year: 2022, "Research on fault early warning of marine diesel engine based on CNN-BiGRU," Journal of Marine Science and Engineering, Vol: 11, No: 1, pp.56.
11. Bingwu Gao; Jing Xu; Zhenrui Zhang; Yanxin Liu; Xiaonan Chang, Year: 2024, "Marine diesel engine piston ring fault diagnosis based on LSTM and improved beluga whale optimization," Alexandria Engineering Journal, Vol: 109, pp. 213-228.
12. Manqi Wang; Hui Cao; Zeren Ai; Qi Zhang, Year: 2024, "Fault diagnosis of ship ballast water system based on support vector machine optimized by improved sparrow search algorithm" Ieee Access, Vol: 12, pp. 17045-17057.